Electrochemically assisted polyamide deposition at three-phase junction

Karolina Sipa, Karolina Kowalewska, Andrzej Leniart, Alain Walcarius, Grégoire Herzog, Slawomira Skrzypek, Lukasz Poltorak

Electrochemistry Communications 123 (2021) 106910

Contents lists available at ScienceDirect

Electrochemistry Communications

journal homepage: www.elsevier.com/locate/elecom

Electrochemically assisted polyamide deposition at three-phase junction

Karolina Sipa [a,*], Karolina Kowalewska [a], Andrzej Leniart [a], Alain Walcarius [b], Grégoire Herzog [b], Sławomira Skrzypek [a], Lukasz Poltorak [a,*]

[a] Department of Inorganic and Analytical Chemistry, Electroanalysis and Electrochemistry Group, Faculty of Chemistry, University of Lodz, Tamka 12, 91-403 Lodz, Poland

[b] Université de Lorraine, CNRS, LCPME, F-54000 Nancy, France

ARTICLE INFO

Keywords:
Electro-assisted deposition
Interfacial polycondensation
Nylon-6,6
Liquid–liquid interface
Polymer
FTO

ABSTRACT

A three-phase junction formed between a solid electrode placed between solutions of the organic phase and the aqueous phase is employed for localized and electrochemically assisted nylon-6,6 deposition. The fluorine-doped tin oxide (FTO) conductive support (serving as the working electrode) is immersed into the cell filled with the aqueous solution of 1,6-hexanediamine (1,6-DAH) and the organic solution of adipoyl chloride (AC) dissolved in 1,2-dichloroethane. The interfacial polycondensation reaction between these two reagents occurs spontaneously at the liquid–liquid interface at elevated pH and is inhibited when diamine is fully protonated. With this in mind, we have designed a system where the pH close to the three-phase junction was increased using electrochemical water reduction triggering very localized polyamide deposition.

1. Introduction

Polyamides (PAs) are polymers which contain recurring amide groups (-CONH-) within the backbone. The most common methods of synthesizing polyamides include polycondensation of (i) dicarboxylic acids with diamines, (ii) dicarboxylic acid chlorides with diamines, (iii) homocondensation of ω-amino acid, and (iv) synthesis from lactanes by their polymerization or hydrolysis to ω-amino acids and further polycondensation [1]. Nylon-6,6 (hexamethylene chain with amide linkages) is one of the most popular polyamides. Nylon finds application as a building block from everyday use objects to labware materials. For the latter, examples include electrode modifiers in supercapacitors [2,3] or in the conventional voltammetric analysis [4,5]. The methods of modification with polyamides developed so far are based on two-stage processing and are carried out *ex situ*, i.e. (i) synthesis of polyamides followed by (ii) their application to various surfaces with electrospray [6], droplet [7], dip [8] or spin coating [9]. In this work, we show that the modifier synthesis and the electrode modification process can be carried out *in situ*, i.e. directly in the measuring vessel triggered by electrochemically controlled pH modulation at the electrode surface.

The electrochemically assisted deposition is an attractive method for the creation of new materials. It involves the electrochemical formation of species that interact with the precursor present near the electrode surface. The electrochemical control eliminates the spontaneous occurrence of the reaction, and thus allows the formation of a precisely defined pattern, shape, size, and location of the structure deposited on the surface of the electrode. A few scenarios can be considered in this respect: (i) anodic dissolution of sacrificial metallic electrodes which causes the formation of metal ions used for the subsequent deposition process [10–12], (ii) electrochemical conversion, in which the produced species catalyze the formation of the deposit (i.e. the electrochemical reduction of Cu^{2+} to Cu^{+}, which is a catalyst in the click chemistry-based surface patterning reactions [13–15]), and finally (iii) local pH changes (production of mesoporous silica [16–18], hydrogels [19,20], titanium dioxide films [21] or mineral (e.g. calcite) surfaces [22,23]).

In electrochemistry, a three-phase junction (solid electrode|water phase|organic phase) is a place where two immiscible phases are contacted to a solid electrode. The latter acts as the working electrode whereas the counter and the reference electrodes are usually placed in the water phase. In such a system, the reaction between reagents separated across the liquid–liquid interface (LLI) is controlled electrochemically only at the location where three phases meet. The three-phase junction is frequently applied to study ionic partitioning between two immiscible phases [24], for purely electroanalytical applications [25] or to electrodeposit solid materials within a defined location (e.g. electrodepositions of gold nanoparticles on tin-doped indium oxide (ITO) [26,27], platinum nanoparticles on fluoride doped indium oxide [28], silica derived from sol-gel processing covering ITO electrode [17,29]).

* Corresponding authors.
E-mail addresses: karolina.sipa@chemia.uni.lodz.pl (K. Sipa), lukasz.poltorak@chemia.uni.lodz.pl (L. Poltorak).

https://doi.org/10.1016/j.elecom.2020.106910
Received 9 December 2020; Received in revised form 20 December 2020; Accepted 21 December 2020
Available online 27 December 2020

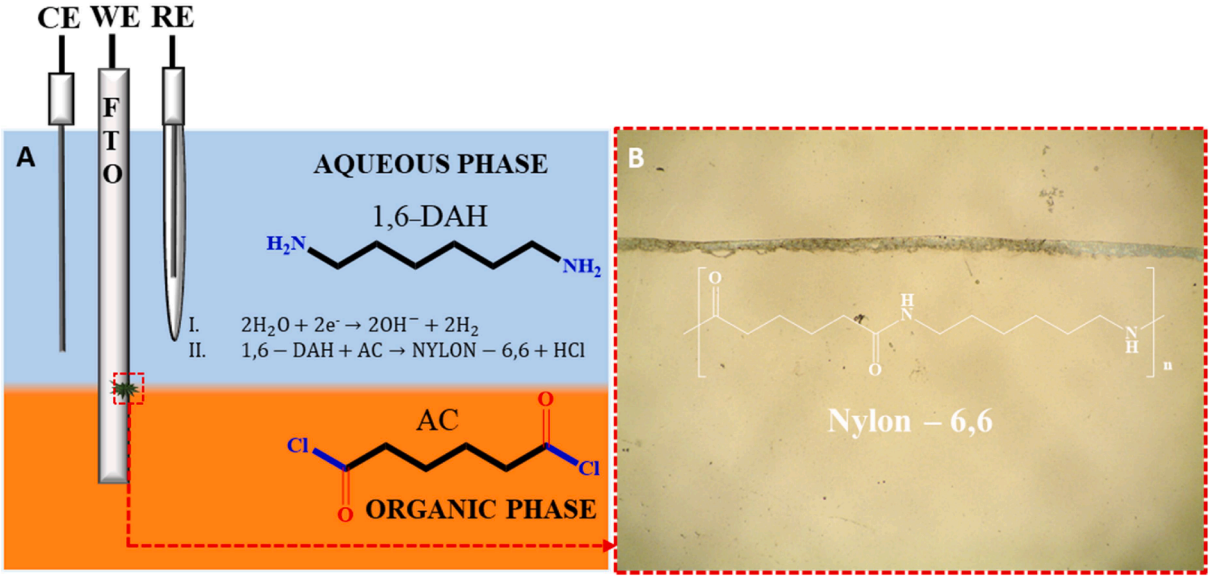

Fig. 1. A. Schematic representation of the electrochemical set-up used to decorate the three-phase junction with polyamide. The reactions I and II were controlled electrochemically. **B.** The optical microscope image of nylon-6,6 stripe formed within the three-phase junction at the FTO electrode (×100 magnitude).

In this work, we wish to report a simple method for the polyamide film formation at the three-phase junction formed between FTO, aqueous solution of 1,6-diaminohexane, and adipoyl chloride dissolved in the 1,2-dichloroethane. The interfacial polycondensation reaction between reagents separated by the LLI occurs only at the three-phase junction and is controlled mainly by the electrochemical water splitting reactions. We have investigated the effect of the experimental conditions and electrochemical processing parameters on the resulting material characteristics. To the best of our knowledge, for the first time, we show the possibility of allowing for the direct, *in situ*, and localized polyamide deposition over conductive support.

2. Material and methods

2.1. Chemicals and reagents

1,6-hexanediamine (1,6-DAH, ≥99.5%, Acros Organics), adipoyl chloride (AC, 98%, Alfa Aesar), 1,2-dichloroethane (1,2-DCE, for analysis, POCh) were used as received. Nitric acid (HNO_3, 65%, Chempur) was used to prepare 0.1 M solution employed for the aqueous phase pH adjustment. All experiments were performed using triple distilled water.

2.2. Instrumentation

Chronoamperometry (CA) and cyclic voltammetry (CV) were performed with a potentiostat EmStat^3 (Palm Instruments B.V., The Netherlands). The FTO electrode (Sigma-Aldrich, surface resistivity ~7 $\Omega \cdot sq^{-1}$), a silver chloride electrode (Ag/AgCl/3M KCl, Mineral, Poland), and a platinum wire (Pt, 99.99%, The Mint of Poland, Warsaw, Poland) served as the working (WE), the reference (RE), and the counter electrode (CE), respectively. The optical microscopy characterization was carried out using a MMT 800BT optical microscope (mikroLAB, Lublin, Poland). The atomic force microscopy (AFM) images were obtained with a Dimension Icon (Bruker, USA) operating in a tapping mode using a commercial scanning probe (TESPA–V2, Bruker, USA). The scanning electron microscopy (SEM) imaging was performed with a JCM-6000 Versatile Benchtop SEM (JEOL, Japan) with an acceleration voltage of 5 kV. IR spectra were recorded in attenuated total reflectance method with Vector 22 PS15 from Bruker.

2.3. Procedures

In all experiments, the WE, CE, and RE were immersed in a voltammetric cell filled with two immiscible liquids as shown in Fig. 1A. WE crossed the LLI whereas CE and RE were only present in the aqueous phase. CV studies were carried out in the potential range from +0.0 V to −1.5 V at the scan rate equal to 100 $mV \cdot s^{-1}$ at different pH of the aqueous phase, as adjusted in the range from 3.0 to 8.5 by the addition of 0.1 M HNO_3 to a solution of 50 mM 1,6-DAH. CA measurements were carried out to investigate the effect of (i) the aqueous phase pH (E = −1.50 V; t = 1800 s; pH = 3.0, 4.5, 6.5, 7.5 or 8.5), (ii) the deposition time (E = −1.50 V; t = 30 s, 60 s, 150 s, 300 s, 600 s or 1800 s; pH = 8.5), and (iii) the potential applied to the working electrode (E = −1.00 V, −1.20 V, −1.30 V, −1.40 V, −1.45 V, −1.50 V, −1.55 V, –1.60 V; t = 150 s; pH = 8.5). Used concentrations of the reagents (1,6-DAH and AC) were chosen based on our previous experience to prevent spontaneous interfacial polycondensation reactions [30].

3. Results and discussion

1,6-DAH is hydrophilic whereas AC is a hydrophobic molecule (theoretical log$P$ values for these compounds equal to −0.2 and 2.0 according to PubChem) [31,32]. It means that these species can only react within the LLI with a thickness defined by the so-called mixed layer region and are not expected to partition to the adjacent phases. The interfacial polycondensation reaction between 1,6-DAH and AC can occur spontaneously at the LLI at elevated pH and is inhibited when diamine is fully protonated ($pKa_1 = 10.8$; $pKa_2 = 11.9$) [33]. With this in mind, we have designed an experimental set-up (Fig. 1A) in which a sufficiently negative potential is applied to the FTO electrode crossing the LLI to enable the reaction occurring in the aqueous phase:

$$2H_2O + 2e^- \rightarrow H_2 + 2OH^- \quad (1)$$

Consequently, the electrochemically formed OH^- ions will be responsible for the local pH increase at the WE surface only on the waterside of the LLI. The section of the WE which is immersed in the denser phase is very well insulated from the CE and RE by resistive 1,2-DCE, and hence, will not experience any applied potential difference. At pH > pK_a both amine groups within 1,6-DAH structure ($pKa_1 = 10.8$; $pKa_2 = 11.9$) [33] initially present in the aqueous phase will deprotonate and will become available to react with AC species from the organic phase.

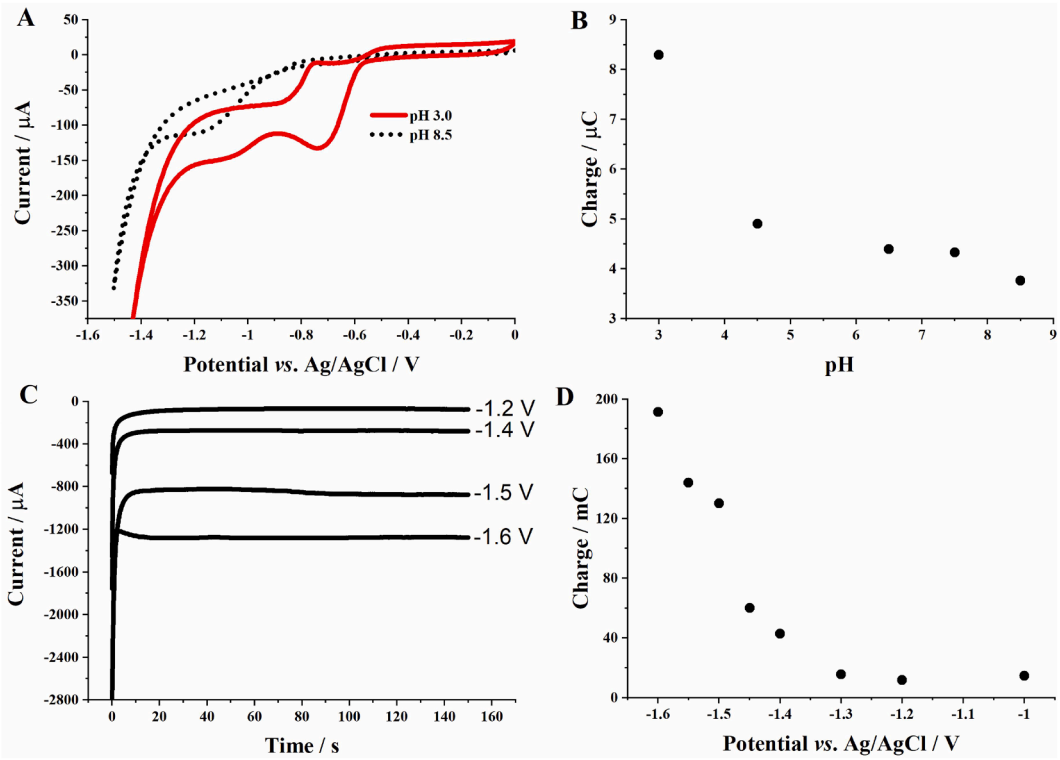

Fig. 2. **A.** CVs recorded at 3.0 and 8.5 pH of the aqueous phase. **B.** The dependence of the transferred charge *vs*. pH of the aqueous phase. **C.** CA recorded at the different applied potential difference values for 150 s at pH 8.5 of the aqueous phase. **D.** The dependence of the transferred charge *vs*. applied potential difference values.

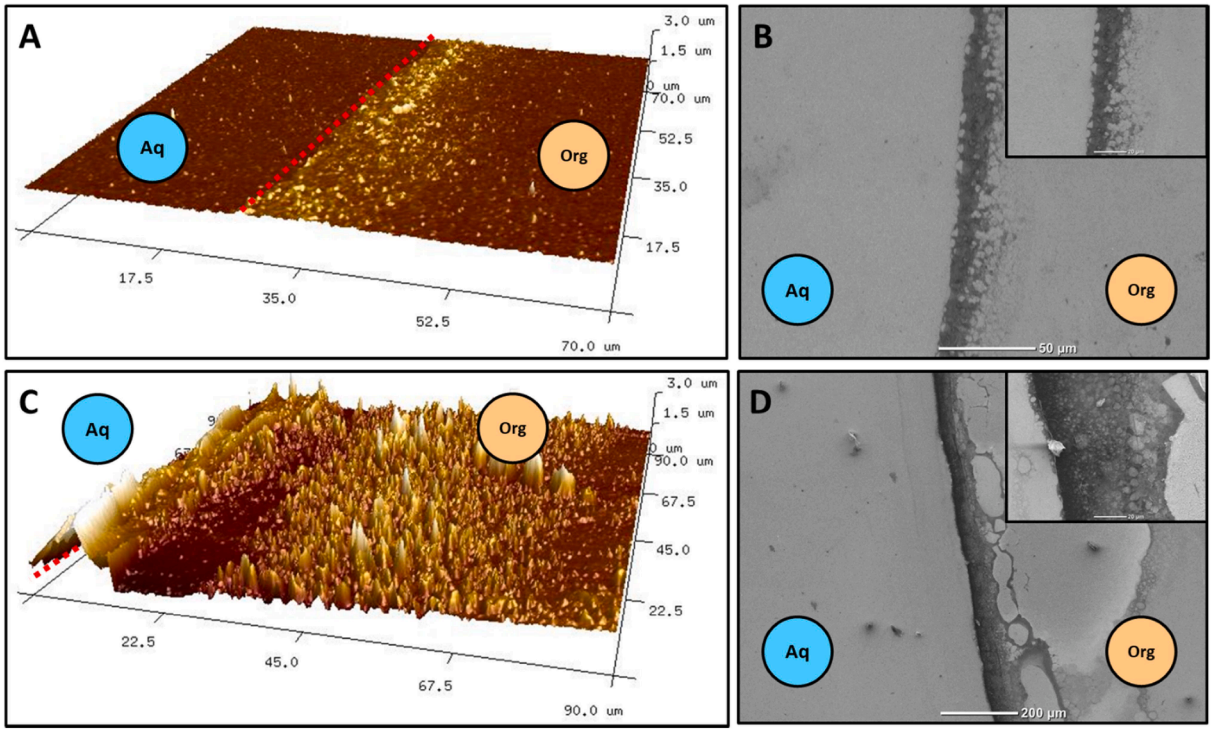

Fig. 3. AFM (A and C) and SEM (B and D together with insets) characterization of the polyamide stripe formed at the three-phase junction during 30 s (A and B) and 600 s (C and D) chronoamperometric deposition at $E = -1.5$ V. For SEM images the scale bars are given at the bottom of each micrography. The red, dashed line indicates the initial position of the three-phase junction. (For interpretation of the references to colour in this figure legend, the reader is referred to the web version of this article.)

$$nH_2N-(CH_2)_6-NH_2+nCl(O)C-(CH_2)_2-C(O)Cl\rightarrow[-OC-(CH_2)_2-CO-NH-(CH_2)_2-NH-]_n+nH^++nCl^- \quad (2)$$

This reaction occurs only at the three-phase junction and is expected to be limited by the diffusion of the non-protonated 1,6-DAH across the alkaline aqueous phase layer adjacent to the FTO surface and AC from the organic phase. Additionally, a small fraction of the H^+ formed as the side product of the interfacial polycondensation reaction can be directly reduced or assist in the reduction of nitrate, further increasing the pH at the three-phase junction:

$$2H^+ + 2e^- \rightarrow H_2 \quad (3)$$

$$NO_3^- + 2H^+ + e^- \rightarrow NO_2 + H_2O \quad (4)$$

Resulting reactions allow for the electrochemically controlled deposition of a polyamide stripe formed at the WE in the very localized position (see Fig. 1B). The nature of the deposit was confirmed by infrared spectroscopy as shown in Fig. S1 and Table S1 available in supporting information. The control experiment was carried out in the same three-phase arrangement without the potential difference applied to the WE. The pH of the aqueous phase was changed by adding 1 M NaOH until the value of pH > 12 was reached. Although thin polyamide film was formed at the LLI, after removing and rinsing the electrode no formation of nylon stripe was observed at its surface even for elongated experimental times.

Fig. 2A shows CVs recorded at FTO immersed into a solution of 50 mM 1,6-DAH (pH = 8.5) and 50 mM 1,6-DAH acidified with 1 M HNO_3 (pH = 3.0). For the latter, as expected, the cathodic current started dropping at around 100 mV higher potential difference value and can be attributed to the reduction of H^+ and NO_3^- (Eqs. (3) and (4), respectively) becoming significant at pH < 4.0 (see Fig. 2B). Fig. 2C and D show CA current patterns and corresponding charge derived from the CA curves integration plotted against applied potential difference values, respectively. Based on this experiment we have chosen $E = -1.5$ V for the three-phase junction decoration being a compromise between possible gas evolution and a sufficient amount of OH^- ion formed at the electrode surface during water reduction reaction. Initial experimental pH = 8.5 is the last point at which the majority of the 1,6-DAH species are fully protonated and any further pH increase will result in the amine groups deprotonation (see concentration fraction diagram from Fig. S2 in supporting information). During electrochemically assisted three-phase junction modification with polyamide deposit, we fixed the concentration of reagents in the aqueous and the organic phase (each 50 mM), pH of the aqueous phase (8.5), and the potential difference value applied to the WE (−1.5 V) to study the effect of the deposition time on the resulting material dimensionality and morphology. The width of the produced nylon stripes can be evaluated from OM, SEM and AFM. We found that longer deposition times allow for the formation of the wider polyamide deposits having μm dimensionality (e.g., average stripe widths of 18 μm and 290 μm for deposition times equal to 30 s and 1800 s were found, respectively).

Fig. 3A and C show the AFM topology images recorded for 30 s and 600 s deposition time. The data for other deposits can be found in supporting information (see Fig. S3 for AFM and Fig. S4 for SEM micrographs). A few interesting conclusions can be drawn from these results: (i) the roughness of the polymeric deposits increases for the longer deposition times (R_q for 1 s = 42.7 ± 3.8 nm, R_q for 30 s = 204.4 ± 41.5 nm – for all values see Fig. S5); (ii) the sharp boundary is always present and is defined by the LLI (it can be observed from the aqueous phase side), and (iii) the width of the diffuse layer growing through the surface of the FTO electrode, penetrates the organic phase and increases at longer deposition time. The asymmetry of the deposit defined by the LLI suggests that the 1,6-DAH transfers to the organic phase close to the three-phase junction as the cathodic potential is being applied to FTO (hydrophobicity of the deprotonated 1,6-DAH species increases, which may result in its spontaneous partition to the organic phase). On the other hand, the deposit widening may be attributed to presumably changing surface wettability affected by the polyamide which in turn may redefine the position of the three-phase junction. In any case, our work offers a very simple procedure allowing for the conductive support modification with a non-redox active polymeric film. In the future, we plan to explore the possibility of the surface patterning with hydrodynamic systems and surfaces with predefined complex wettability patterns.

4. Conclusions

In this work, we show that the electrochemically controlled pH increase within the three-phase junction can be used to directly modify a solid electrode with electrochemically inactive polyamide material. Our electrochemical configuration (solid electrode crossing LLI) allowed for the localized deposition of the polyamide stripe with the thickness controlled by the deposition time or the cathodic potential difference applied to the working electrode surface. Our protocol can be extended to other than nylon-6,6 polyamides. Proper arrangement of the LLI and the solid electrode may be further harvested to define different geometries (thin films, rings, patterns) of a final deposit.

CRediT authorship contribution statement

Karolina Sipa: Conceptualization, Methodology, Formal analysis, Writing - original draft. **Karolina Kowalewska:** Formal analysis. **Andrzej Leniart:** Formal analysis. **Alain Walcarius:** Writing - review & editing, Supervision. **Grégoire Herzog:** Writing - review & editing, Supervision. **Sławomira Skrzypek:** Writing - review & editing, Supervision. **Lukasz Poltorak:** Conceptualization, Methodology, Formal analysis, Writing - original draft, Funding acquisition, Project administration, Supervision.

Declaration of Competing Interest

The authors declare that they have no known competing financial interests or personal relationships that could have appeared to influence the work reported in this paper.

Acknowledgements

This project was financially supported by the National Science Center (NCN) in Krakow, Poland (Grant no. UMO-2018/31/D/ST4/03259). K.S. is grateful to Campus France, France for financing her BGF séjour de recherche.

Appendix A. Supplementary data

Supplementary data to this article can be found online at https://doi.org/10.1016/j.elecom.2020.106910.

References

[1] K. Piradashvili, E.M. Alexandrino, F.R. Wurm, K. Landfester, Reactions and Polymerizations at the Liquid–Liquid Interface, Chem. Rev. 116 (4) (2016) 2141–2169, https://doi.org/10.1021/acs.chemrev.5b00567.

[2] S. Palsaniya, H.B. Nemade, A.K. Dasmahapatra, Hierarchical Nylon-6/reduced graphene oxide/polyaniline nanocomposites with enhanced dielectric properties for energy storage applications, J. Storage Mater. 32 (2020) 101821, https://doi.org/10.1016/j.est.2020.101821.
[3] X. Zhang, M. Gao, L. Tong, K. Cai, Polypyrrole/nylon membrane composite film for ultra-flexible all-solid supercapacitor, J. Materiomics 6 (2) (2020) 339–347, https://doi.org/10.1016/j.jmat.2019.11.004.
[4] P. Thanalechumi, A.R.M. Yusoff, Z. Yusop, Novel Electrochemical Sensor Based on Nylon 6,6-Modified Graphite HB Pencil Electrode for Chlorothalonil Determination by Differential Pulse Cathodic Stripping Voltammetry, Water Air Soil Pollut. 231 (5) (2020), https://doi.org/10.1007/s11270-020-04536-8.
[5] O.E. Fayemi, A.S. Adekunle, E.E. Ebenso, A Sensor for the Determination of Lindane Using PANI/Zn, Fe(III) Oxides and Nylon 6,6/MWCNT/Zn, Fe(III) Oxides Nanofibers Modified Glassy Carbon Electrode, J. Nanomater. 2016 (2016) 1–10, https://doi.org/10.1155/2016/4049730.
[6] J. Kratochvíl, D. Kahoun, O. Kylián, J. Štěrba, T. Kretková, J. Kousal, J. Hanuš, J. Vaclová, V. Prysiazhnyi, P. Sezemský, P. Fojtíková, J. Lieskovská, H. Langhansová, I. Krakovský, V. Straňák, Nitrogen enriched C:H:N:O thin films for improved antibiotics doping, Appl. Surf. Sci. 494 (2019) 301–308, https://doi.org/10.1016/j.apsusc.2019.07.135.
[7] P. Thanalechumi, A.R. Mohd Yusoff, Z. Yusop, Nylon 6,6 modified screen printed carbon electrodes as electrochemical sensors for rapid chlorothalonil determination in water samples using differential pulse cathodic stripping voltammetry, J. Environ. Sci. Health, Part B 54 (4) (2019) 294–302, https://doi.org/10.1080/03601234.2018.1561057.
[8] P. Thanalechumi, A.R. Mohd Yusoff, Z. Yusop, Green sensors for voltammetric determination of lindane in water samples using bare and nylon 6,6 modified pencil electrodes, Anal. Methods 11 (38) (2019) 4899–4909, https://doi.org/10.1039/C9AY01589B.
[9] N. Tsutsumi, N. Kajimoto, K. Kinashi, W. Sakai, Understanding ferroelectric performances of spin-coated odd–odd nylon thin films, J. Appl. Polym. Sci. 136 (2019) 1–11, https://doi.org/10.1002/app.47595.
[10] V. Badets, D. Duclos, D. Quinton, O. Fontaine, D. Zigah, Original Dual Microelectrode: Writing and Reading a local click reaction with Scanning Electrochemical Microscopy, Electrochim. Acta 201 (2016) 274–278, https://doi.org/10.1016/j.electacta.2015.10.066.
[11] R. Ameloot, L. Stappers, J. Fransaer, L. Alaerts, B.F. Sels, D.E. De Vos, Patterned Growth of Metal-Organic Framework Coatings by Electrochemical Synthesis, Chem. Mater. 21 (13) (2009) 2580–2582, https://doi.org/10.1021/cm900069f.
[12] S. Sachdeva, M.R. Venkatesh, B.E. Mansouri, J. Wei, A. Bossche, F. Kapteijn, G. Q. Zhang, J. Gascon, L.C.P.M. de Smet, E.J.R. Sudhölter, Sensitive and Reversible Detection of Methanol and Water Vapor by In Situ Electrochemically Grown CuBTC MOFs on Interdigitated Electrodes, Small 13 (29) (2017) 1604150, https://doi.org/10.1002/smll.201604150.
[13] J. Matyjewicz, A. Lesniewski, J. Niedziolka-Jonsson, Click chemistry modification of glassy carbon electrode with gold nanoparticles for electroactive ion discrimination, Electrochem. Commun. 48 (2014) 73–76, https://doi.org/10.1016/j.elecom.2014.08.020.
[14] S.-Y. Ku, K.-T. Wong, A.J. Bard, Surface Patterning with Fluorescent Molecules Using Click Chemistry Directed by Scanning Electrochemical Microscopy, J. Am. Chem. Soc. 130 (8) (2008) 2392–2393, https://doi.org/10.1021/ja078183d.s002.
[15] D. Quinton, A. Maringa, S. Griveau, T. Nyokong, F. Bedioui, Surface patterning using scanning electrochemical microscopy to locally trigger a “click” chemistry reaction, Electrochem. Commun. 31 (2013) 112–115, https://doi.org/10.1016/j.elecom.2013.03.021.
[16] A. Walcarius, E. Sibottier, M. Etienne, J. Ghanbaja, Electrochemically assisted self-assembly of mesoporous silica thin films, Nat. Mate.r 6 (8) (2007) 602–608, https://doi.org/10.1038/nmat1951.
[17] J. Niedziolka-Jonsson, M. Jonsson-Niedziolka, W. Nogala, B. Palys, Electrosynthesis of thin sol–gel films at a three-phase junction, Electrochim. Acta 56 (9) (2011) 3311–3316, https://doi.org/10.1016/j.electacta.2011.01.024.
[18] G. Giordano, N. Vilà, E. Aubert, J. Ghanbaja, A. Walcarius, Multi-layered, vertically-aligned and functionalized mesoporous silica films generated by sequential electrochemically assisted self-assembly, Electrochim. Acta 237 (2017) 227–236, https://doi.org/10.1016/j.electacta.2017.03.220.
[19] R. Fernandes, L.-Q. Wu, T. Chen, H. Yi, G.W. Rubloff, R. Ghodssi, W.E. Bentley, G. F. Payne, Electrochemically Induced Deposition of a Polysaccharide Hydrogel onto a Patterned Surface, Langmuir 19 (10) (2003) 4058–4062, https://doi.org/10.1021/la027052h.
[20] V. Lakshminarayanan, L. Poltorak, E.J.R. Sudhölter, E. Mendes, J. van Esch, Electrochemically assisted hydrogel deposition, shaping and detachment, Electrochim. Acta 350 (2020) 136352, https://doi.org/10.1016/j.electacta.2020.136352.
[21] A. Naldoni, A. Minguzzi, A. Vertova, V.D. Santo, L. Borgese, C.L. Bianchi, Electrochemically assisted deposition on TiO 2 scaffold for Tissue Engineering: an apatite bio-inspired crystallization pathway, J. Mater. Chem. 21 (2) (2011) 400–407, https://doi.org/10.1039/C0JM02446E.
[22] E.A. Kulp, J.A. Switzer, Electrochemical biomineralization: The deposition of calcite with chiral morphologies, J. Am. Chem. Soc. 129 (2007) 15120–15121, https://doi.org/10.1021/ja076303b.
[23] R. Haaring, N. Kumar, D. Bosma, L. Poltorak, E.J.R. Sudhölter, Electrochemically Assisted Deposition of Calcite for Application in Surfactant Adsorption Studies, Energy Fuels 33 (2) (2019) 805–813, https://doi.org/10.1021/acs.energyfuels.8b03572.s001.
[24] R. Gulaboski, V. Mireski, F. Scholz, An electrochemical method for determination of the standard Gibbs energy of anion transfer between water and *n*-octanol, Electrochem. Commun. 4 (4) (2002) 277–283, https://doi.org/10.1016/S1388-2481(02)00264-3.
[25] R.S. Vishwanath, E. Witkowska Nery, M. Jönsson-Niedziółka, Electrochemistry of selected quinones at immiscible n-octyl-2-pyrrolidone/aqueous interface using a three-phase electrode system, Electrochim. Acta 306 (2019) 54–60, https://doi.org/10.1016/j.electacta.2019.03.095.
[26] I. Kaminska, J. Niedziolka-Jonsson, A. Roguska, M. Opallo, Electrodeposition of gold nanoparticles at a solid|ionic liquid|aqueous electrolyte three-phase junction, Electrochem. Commun. 12 (12) (2010) 1742–1745, https://doi.org/10.1016/j.elecom.2010.10.011.
[27] I. Kaminska, M. Jonsson-Niedziolka, A. Kaminska, M. Pisarek, R. Hołyst, M. Opallo, J. Niedziolka-Jonsson, Electrodeposition of Well-Adhered Multifarious Au Particles at a Solid|Toluene|Aqueous Electrolyte Three-Phase Junction, J. Phys. Chem. C 116 (42) (2012) 22476–22485, https://doi.org/10.1021/jp307674k.
[28] V.A. Online, V. Lakshminarayanan, L. Poltorak, D. Bosma, E.J.R.R. Sudhölter, J. H. van Esch, E. Mendes, Locally pH controlled and directed growth of supramolecular gel microshapes using electrocatalytic nanoparticles, Chem. Commun. 55 (2019) 9092–9095, https://doi.org/10.1039/c9cc04238e.
[29] K. Szot, M. Jönsson-Niedziolka, B. Palys, J. Niedziolka-Jönsson, One-step electrodeposition of carbon–silicate sponge assisted by a three-phase junction for efficient bioelectrocatalysis, Electrochem. Commun. 13 (6) (2011) 566–569, https://doi.org/10.1016/j.elecom.2011.03.011.
[30] K. Kowalewska, K. Sipa, A. Leniart, S. Skrzypek, L. Poltorak, Electrochemistry at the liquid–liquid interface rediscovers interfacial polycondensation of nylon-6,6, Electrochem. Commun. 115 (2020) 106732, https://doi.org/10.1016/j.elecom.2020.106732.
[31] PubChem - 1,6-hexanediamine, (n.d.). https://pubchem.ncbi.nlm.nih.gov/compound/1_6-Hexanediamine#section=Depositor-Supplied-Synonyms (accessed October 23, 2020).
[32] PubChem - Adipoyl chloride, (n.d.). https://pubchem.ncbi.nlm.nih.gov/compound/Adipoyl-chloride#section=Depositor-Supplied-Synonyms (accessed October 23, 2020).
[33] D.R. Lide, CRC Handbook of Chemistry and Physics, 84th Edition, 2003-2004, Handb. Chem. Phys. 53 (2003) 2616.